Supporting Information

One-step catalytic amination of naphthalene to naphthylamine with exceptional yield

Fang Hao, Xin Wang, Linfang Huang, Wei Xiong*, Pingle Liu*, He'an Luo

Abstract:

One-step amination of aromatic compounds to arylamine is a promising process with high atom utilization and less environmental pollution. We first propose a direct catalytic amination of naphthalene to naphthylamine with hydroxylamine by using vanadium catalysts under mild conditions. A naphthylamine yield of 70% was achieved over V_2O_5/HZSM-5 cayalyst in one-step amination of naphthalene, which is higher than the state-of-art processes. The Brönsted acid sites and the V-O-V and V=O bonds of monovanadate on V_2O_5/HZSM-5 catalyst are the active sties of the amination reaction and responsible for the naphthalene activation and the formation of NH_3^+ that acts as the active amination reagent. A possible reaction mechanism was also proposed by investigating real-time IR and in-situ DRIFTs. This proposed one-step amination of naphthalene is superior to traditional un-selective nitration and hydrogenation processes, and some findings offer new insights to produce arylamine from aromatic compounds.

DOI: 10.1002/anie.2020XXXXX

SUPPORTING INFORMATION

Experimental Procedures

Materials

Analytical-grade NH_4VO_3 (Macklin Biochemical, 99%), V_2O_5 (Jinshan Chemical, 99%), and $NH_2OH{\cdot}HCl$ (Macklin Biochemical, 98.5%) were commercially obtained. The glacial acetic acid (XiLong Chemical, >99%) and naphthalene (Guangfu-chem, 99%) were of analytical grade and used without further purification. TiO_2 and SiO_2 were purchased from Chengdu Organic Chemicals Co., Ltd. Chinese Academy of Sciences. MCM-41 and HZSM-5 were purchased from Liyuan New Science and Technology Chemical Materials Management Department.

Catalyst preparation

The supported vanadium oxide catalysts, V_2O_5/TiO_2, V_2O_5/SiO_2, V_2O_5/MCM-41, and V_2O_5/HZSM-5 were prepared by impregnation of different support with an aqueous solution of NH_4VO_3 heat, stir and dry in an 80 °C water bath and then calcination for 1 hour at 100 °C and 4 hours at 500 °C.

Amination reaction test

The amination reaction was carried out at atmospheric pressure by using naphthalene and $NH_2OH{\cdot}HCl$ as raw materials together with the vanadium-based catalyst in acidic medium solution. Considering that naphthalene is easy to sublimate and could condense into solid naphthalene during the reaction when the naphthalene was fed by disposable batch feeding mode. Therefore, the feeding mode of naphthalene was also investigated and the experimental steps are as follows:

For the naphthalene disposable batch feeding mode, 0.78 mmol of naphthalene, 7.8 mmol $NH_2OH{\cdot}HCl$ and 0.5g of catalyst were sequentially added to a two-necked flask with a certain volume of 15ml of HOAc and 5ml of water. After all of the reactant was added, the two-necked flask was placed in a collecting thermostatic heating magnetic stirrer and fixed. The thermometer was then inserted and a reflux condenser was installed, the reactant mixture was gradually heated to 80°C. At this temperature, the mixture was stirred and refluxed for 4h.

For the intermittent feeding mode, the naphthalene solution dissolved in acetic acid-aqueous was intermittently added in the reactant mixture of 0.5g of catalyst and acetic acid-aqueous dissolved 7.8 mmol $NH_2OH{\cdot}HCl$ in a two-necked flask at 80°C. The duration time of naphthalene solution introduction were controlled at 20, 30 and 40 minutes, respectively.

Catalyst characterization methods

BET analysis: The BET surface area was calculated from the N_2 adsorption data that were obtained using a PLUS HD88/ASAP 2020 apparatus (Micromeritics Instruments Corporation) at liquid N_2 temperature.

X-ray diffraction (XRD) analysis: Crystallographic analysis of the tested catalysts was performed by means of X-ray diffraction (XRD) measurements in θ–2θ mode using an Ultima 4 apparatus with lynx eye detector covering 5° and 100° with a step of 0.02°.

Transmission electron microscope (TEM) analysis: The metal dispersion, particle size, and lattice of the prepared materials were analyzed by Jeol 2100F transmission electron microscope.

NH_3-Temperature-programmed desorption (NH_3-TPD): All the catalysts were carried out on a ChemBET300 were carried out by pre-treating the samples from room temperature to 700°C under a helium flow rate of 100 ml min^{-1}.

Raman spectra analysis: Laser-Raman spectra were obtained using a Renishaw inVia instrument the samples were excited with the 532 nm Ar line under N_2 atmosphere**.**

Pyridine-IR analysis: The samples were monitored on a Hicube80 + Nicoletis spectrometer using self-supporting wafers in a heatable IR gas cell.

ATR analysis: Analysis of functional groups of reactants solution were detect by using React ATR on Nicolet iS10 (FT-IR) spectrometer with scanning speed in 40 spectra per second and measurements from 500 cm^{-1} to 4000 cm^{-1}.

EPR spectra: The X-band EPR spectra were obtained on a JEOL FA300 spectrometer, operating at 9.06GHz, modulation frequency, 100.00 kHz; modulation amplitude, 1.00 G; time constant, 0.03s; sweep time, 2min; and trapping agent, PBN. All the texts were under reaction condition. The g values were determined by simulating the spectra using JEOL ESR DP.

In-situ analysis measurement

Real-*time* IR analysis: The *real-time* IR measurements were carried out using React ATR-Probe IN350- TEX equipment (BRUKER) with a light conduit and diamond insertion probe. The system of MCT (Mercury cadmium telluride) was cooled using liquid N_2. FTIR spectra were collected in the wave number range between 3000 and 650 cm^{-1}. The experiments were performed at 80 °C in a 100 mL, 3-necked flask with a condenser, thermometer, and magnetic stirrer. The temperature was maintained by using an appropriately adjusted oil bath. The amount of each substance was 0.78mmol naphthalene; 0.5g catalysts; 7.2mmol $NH_2OH{\cdot}HCl$; 15ml HOAc; 5ml H_2O; Catalyst: 3% V_2O_5/HZSM-5. The ReactIR15 probe was stretched into the liquid system and scanned every 15s.

***In-situ* DRIFTs analysis:** *In-situ* Diffuse Reflectance Infrared Fourier Transform Spectroscopy (*In-situ* DRIFTS) study was conducted on iS50 equipped with an in-situ DRIFTS cell and a mercury-cadmium-telluride MCT detector cooled by liquid N_2. All samples adsorbed naphthalene and hydroxylamine hydrochloride in the molar ratio of 1:10 at room temperature. The samples were pretreated at room temperature for 30 min under N_2 stream, warmed to 120 °C, and collect background at each temperature interval under N_2, the temperature is increased from 40 °C to 120 °C with a heating rate of 10 °C/min, and the spectra were measured every 2 min.

Results and Discussion

XRD

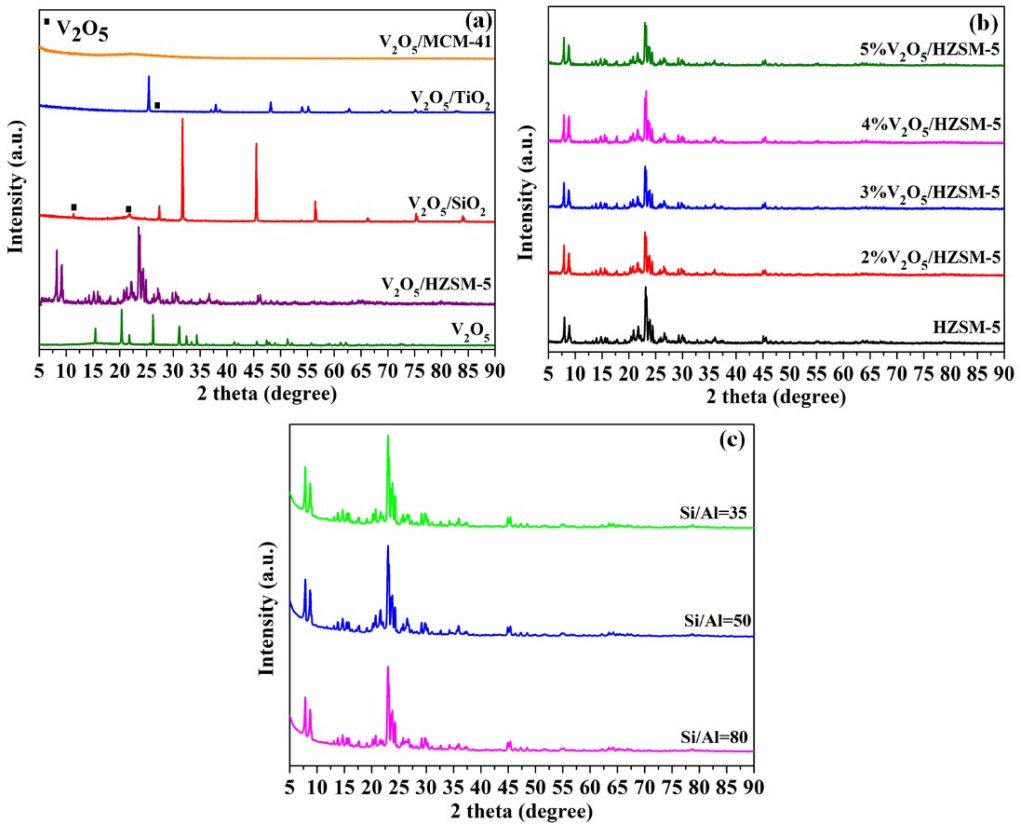

Figure S1. XRD diffraction spectra of different supported catalysts: (a) Different supported vanadium oxide catalysts with V_2O_5 loading of 2%; (b) V_2O_5/HZSM-5 with different vanadium oxide loading; (c) 2% V_2O_5/HZSM-5 with different Si/Al ratio

The XRD of different supported catalysts under the same vanadium oxide loading (2%) were tested. The results are shown in **Figure S1a**. The weak the characteristic peaks of vanadium oxide were detected on the supported catalysts with SiO_2 and TiO_2. While there were not obvious vanadium oxide diffraction peaks detected on the supported catalysts of MCM-41 and HZSM-5. It indicates that the vanadium species have better dispersion on the supported of MCM-41 and HZSM-5 with the same metal loading contents.

The XRD of different vanadium oxide loading on HZSM-5 and different Si/Al ratio with same 2% loading of vanadium oxide was also characterized by XRD. The results are shown in **Figure S1b** and **c**. All the catalysts show the strong intensity of the characteristic peaks in the XRD patterns, suggesting that the introduction of vanadium oxide on the HZSM-5 did not obviously reduce the crystalline structure of the HZSM-5 zeolites. It is observed that the characteristic diffraction peaks at 2θ=7°-9° and 2θ=23°-25° are observed which attributed to the HZSM-5 zeolite.[1] Moreover, the characteristic diffraction peaks of vanadium oxide did not appear on the catalyst with vanadium content less than 5% and there is no evident peak to be indicative of the presence of impurities. So it could be concluded that vanadium species are highly dispersed on the surface of HZSM-5 support.

NH_3-TPD

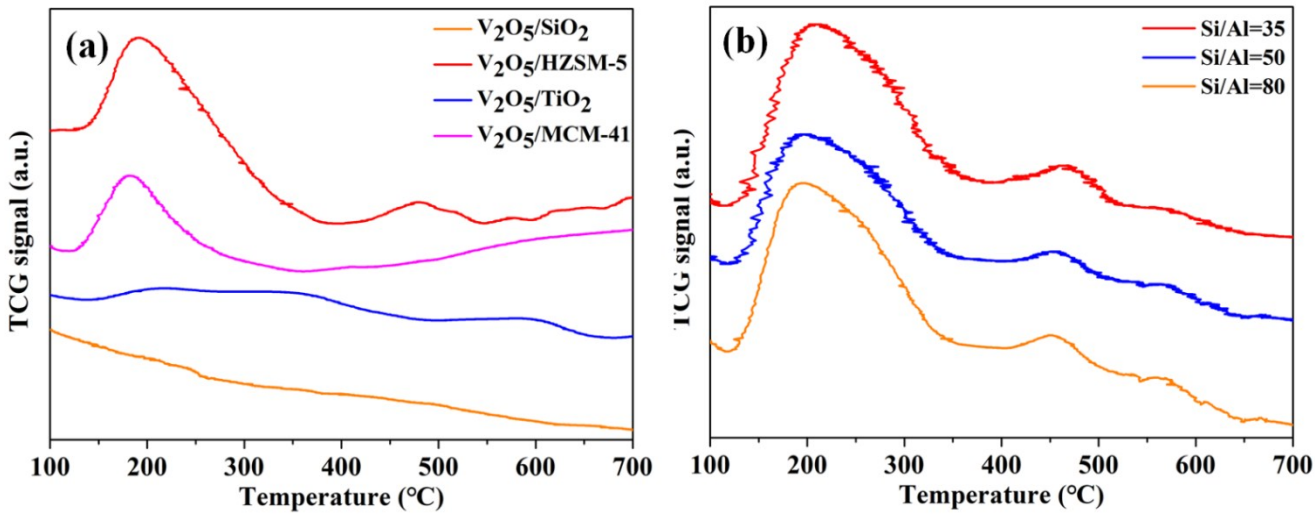

Figure S2. NH_3-TPD of different supported 2% vanadium oxide catalysts (a); and 2% V_2O_5/HZSM-5 with different Si/Al ratios (b)

NH_3-TPD was performed in order to investigate the influence of acidity on the catalytic reactions, and the results are shown in **Figure S2a**. It can be seen that the HZSM-5 supported catalyst displayed a shoulder at 510–560 °C corresponding to acid sites with medium strength along with the main peak ascribed to weak sites at 205–215 °C. And for MCM-41, TiO_2 only showed a shoulder at around 200 °C corresponding to weak strength of acid sites. It has been reported that the formation of products is closely related to the interaction of reactants or intermediates produced on the MCM-41 supported vanadium catalysts with surface medium acid sites during the reaction.[2]

NH_3-TPD experiments were also carried out for investigating the acidity of 2% V_2O_5/HZSM-5 with different ratios of Si/Al. All the catalysts have two ammonia desorption peaks. According to **Figure S2b**, the first peak for HZSM-5 is achieved at about 180 °C, which is associated with weak acid sites. The second peak is obtained at around 400 °C, which is associated with strong acid sites. The peak at the low temperature (around 180 °C) is assigned as that of ammonia adsorbed on non-acidic OH groups or ammonium cations that formed by the reaction of Lewis acid sites, whereas the peak at higher temperature (around 400 °C) is assigned as the desorption peak of ammonia adsorbed on the Brönsted acid sites.[3,4] With the increase of the Si/Al ratio, the acid properties of the catalysts will be lower with the two peaks decrease as the Si/Al ratio increasing.

Pyridine-IR

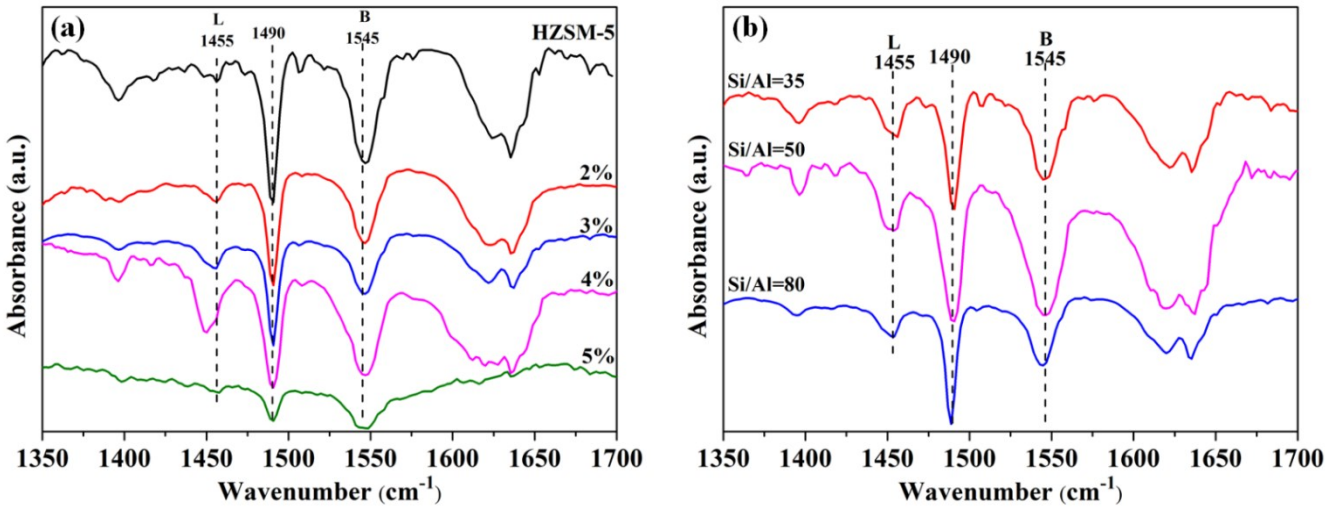

Figure S3. Py-IR of V_2O_5/HZSM-5 with different vanadium oxide loading (a); and 2% V_2O_5/HZSM-5 different Si/Al ratio (b)

In the spectrum of the samples, the bands around 1455 cm^{-1} appeared and corresponded to the Lewis acid sites.[3, 4] The band at 1545 cm^{-1} can be attributed to the Brönsted acid sites.[5] Addition bands at 1490 and around 1600-1650 cm^{-1}, associated with the presence of pyridine, are also observed in all supported catalysts, indicating that the change of vanadium loading and Si/Al ratio can not change the properties and proportion of acid sites in the catalyst.

ATR analysis

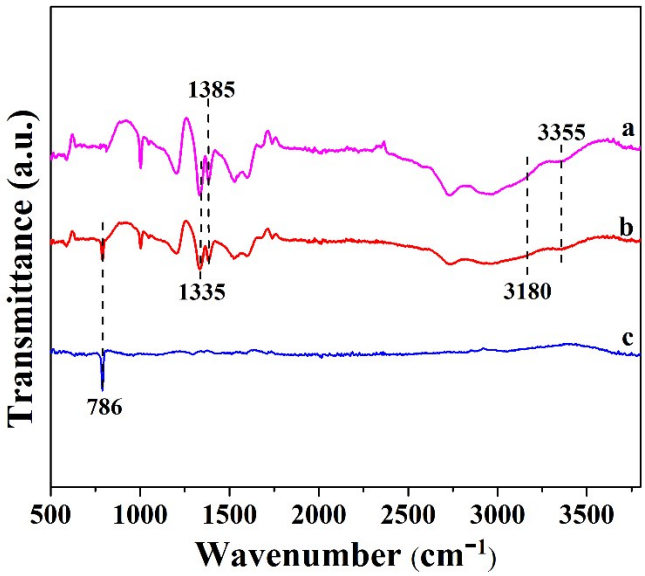

Figure S4. ATR spectra of reaction system: (a) hydroxylamine hydrochloride; (b) the mixture of hydroxylamine hydrochloride and naphthalene; (c) naphthalene.

The ATR spectra of the naphthalene, hydroxylamine hydrochloride and their mixture are shown in **Figure S4.** The background of acetic acid-water has been deducted. The characteristic peak of 786 cm^{-1} belongs to the naphthalene. The characteristic bands of 1335 and 1385 cm^{-1} are ascribed to the $–(NH_3OH)^+$, and the peaks of 3180 and 3350 cm^{-1} are assigned to dissociative $-NH_2$.[6] The characteristic peaks of wavenumbers from 600 to 2400 cm^{-1} in the reactant mixture of hydroxylamine hydrochloride and naphthalene (Figure S4b) is as same as the characteristic peaks in *Real-time* IR before the reaction. Moreover, the characteristic peak of $-NH_3^+$ was not detected in the reactant mixture before reaction proceeding, which indicate that the $-NH_3^+$ are mainly formed during the one-step naphthalene amination reaction.

***Real-time* IR result**

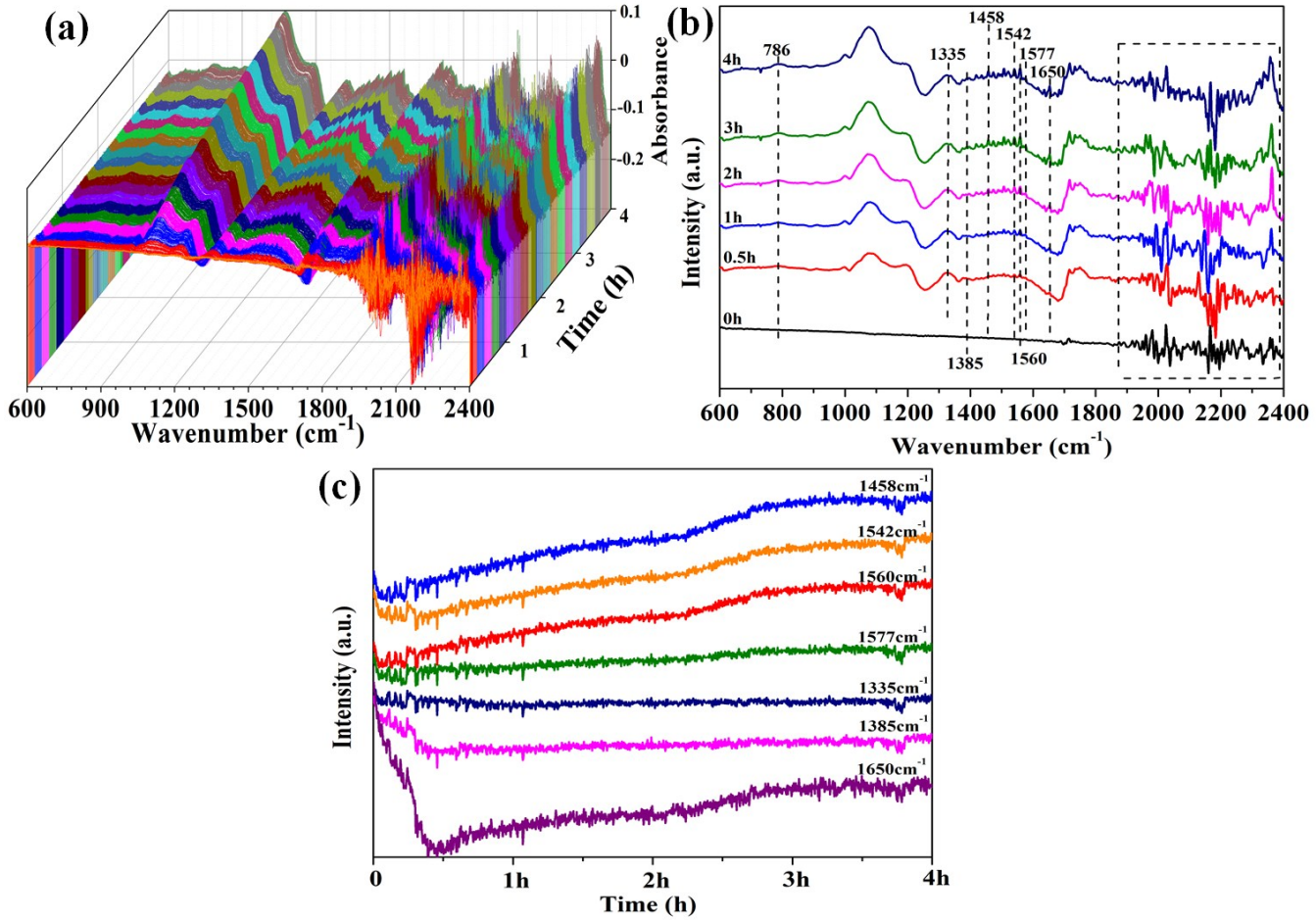

Figure S5. *Real-time* IR of disposable batch feeding mode: (a) Real-time IR spectrum; (b) Characteristic peaks of functional groups; (c) Intensity changes of functional groups

The *Real-time* IR spectrum of the disposable batch feeding operation is shown in **Figure S5.** The diffraction peak of 786 cm^{-1} belongs to the naphthalene, and the diffraction peak of 1577cm^{-1} belongs to the $-NH_3^+$. The diffraction peaks of 1458, 1542 and 1560cm^{-1} belong to AR-NH_2. And the diffraction bands of 1335 and 1385 cm^{-1} belongs to $-(NH_3OH)^+$.[6] The peak of $-NH_3^+$ increased gradually at first and then remained stable. The diffraction peak of AR-NH_2 shows the same trend but it is more obvious than intermittent feeding. In addition, there's been a peak at 1650cm^{-1} belonged to amido. This indicated that naphthylamines could also react with acetic acid to form amides in the reaction system.

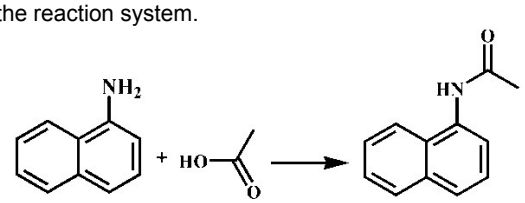

EPR spectra

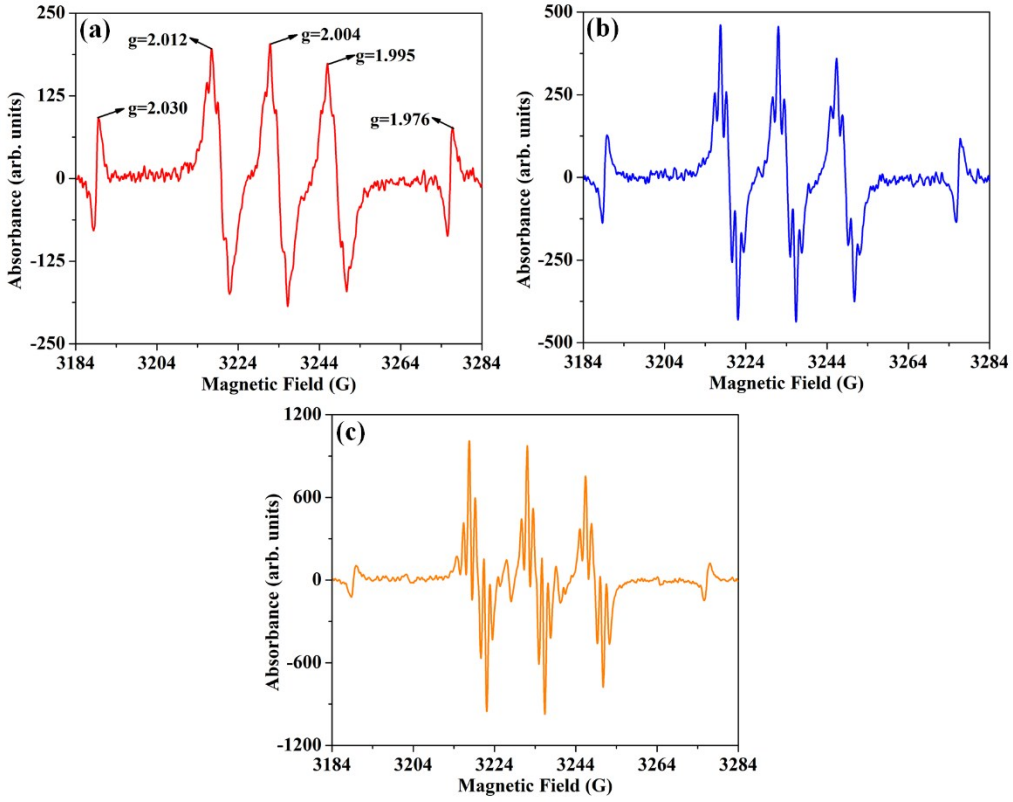

Figure S6 EPR spectra of reaction system in different time: (a) 0h; (b) 1h; (c) 2h

The EPR spectra of reaction system in different time are shown in the **Figure S6**. It can be seen that the EPR signal enhanced gradually with the increasing of reaction time. At the beginning of the reaction, three strong EPR signals appear in the reaction system at g =2.012, 2.004 and 1.995. And the other two weak EPR signals appear at g=1.976 and 2.030. These signals belong to naphthalene. When the reaction lasted for 1 hour, several new free radical peaks appeared, which results from the activation of naphthalene. When the reaction lasted for 2 hours, a typical EPR signal of naphthalene free radical was detected[7]. The naphthalene free radical species could be formed efficiently during the reaction. Combining with Real-time IR (Figure 4 and S4) -NH_3^+ free radical was detected and the reaction time between 1 to 2 h is the fast time for Ar-NH_2 production. It indicates that sufficient radicals could be stable and be detected in the reaction solution under the present conditions.

TEM

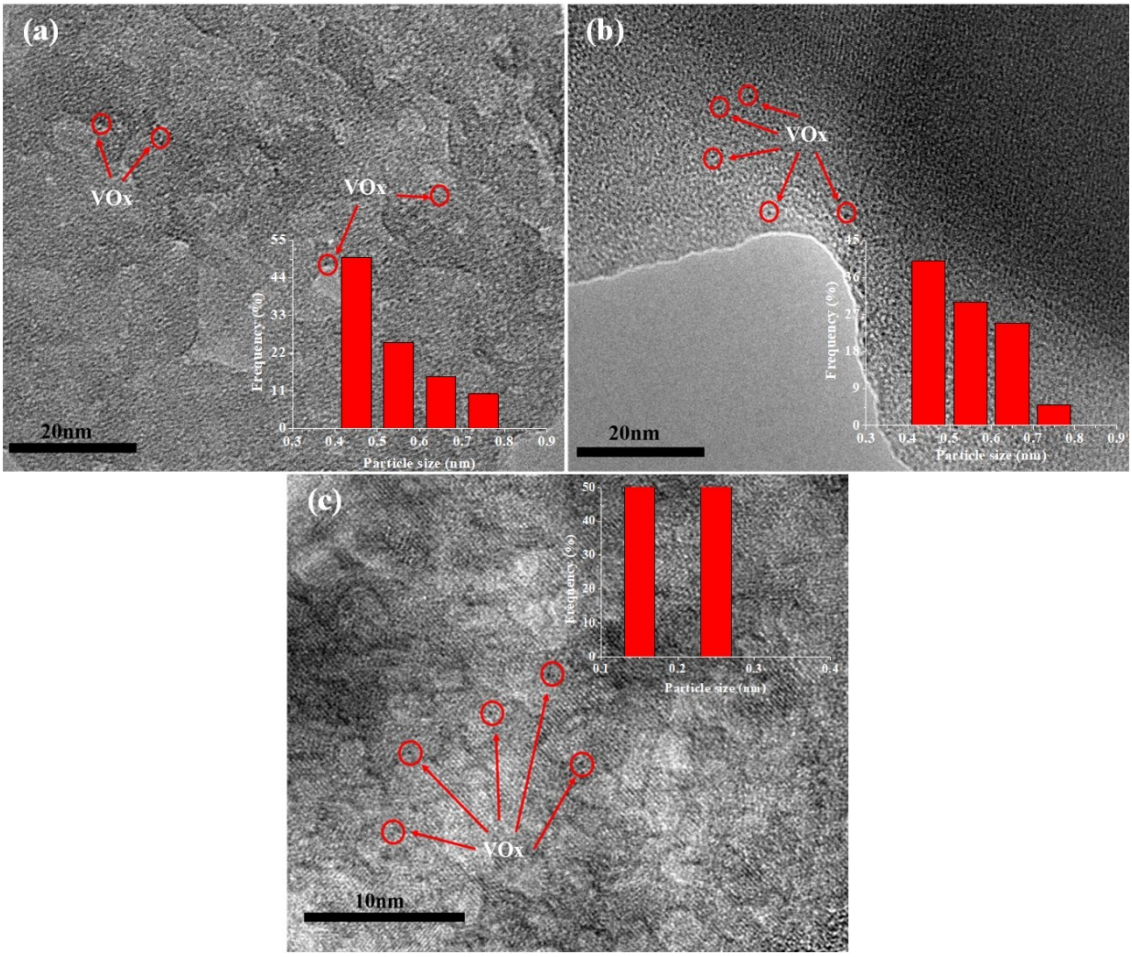

Figure S7. TEM of different catalysts: (a) V_2O_5/MCM-41; (b) V_2O_5/SiO_2; (c) V_2O_5/TiO_2

The TEM of different supported catalytic was carried out and shown in **Figure S7**. All the results were 2% vanadium oxide content. It can be seen clearly that the particle size is homogeneous and very fine.

Raman results

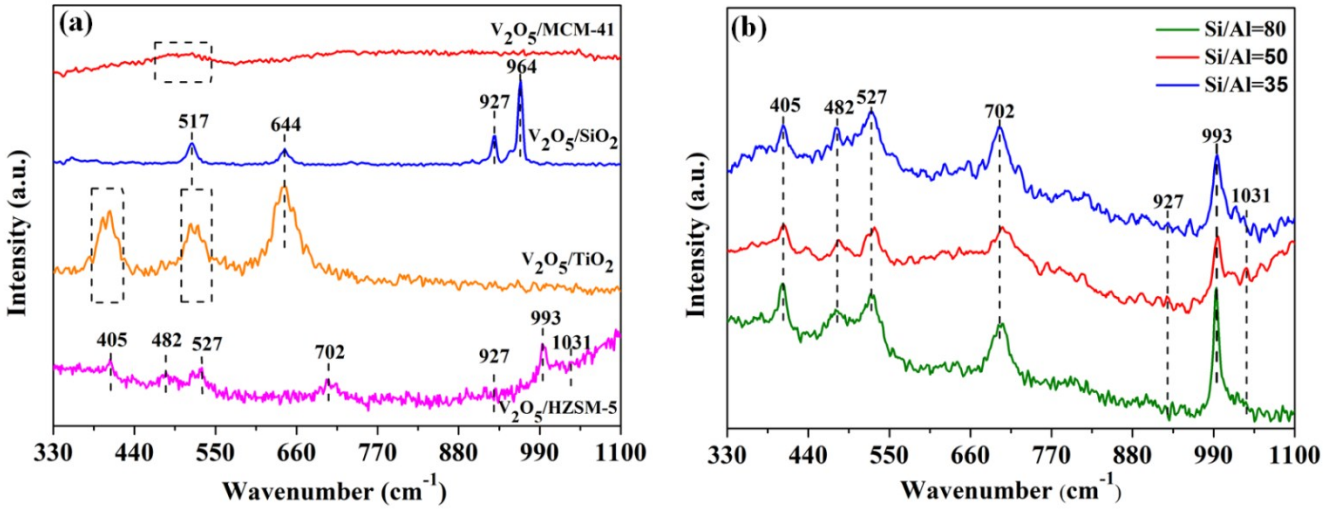

Figure S8. Raman of different supported catalysts with 2% V_2O_5 loading content (a); and /HZSM-5 with different Si/Al ratio (b)

Figure S8a shows Raman spectroscopy results of different supported catalysts. The broad bands at 490 and 610 cm^{-1} for V_2O_5/MCM-41 are attributed to the 3 and 4 Si siloxane rings.[8] In addition, there are no additional characteristic bands of V_2O_5/MCM-41 belonging to vanadium species, which means that the Raman bands related to vanadium species in MCM-41 are too weak to be detected by visible Raman spectroscopy.[9] By contrast, it shows obviously bands at 517 and 644 cm^{-1} belonging to the vibration of V_2O_5 crystallites in V_2O_5/SiO_2.[10] The diffraction band of 927cm^{-1} is attributed to the polymerized V-O-V structure.[4,11] Raman bands centered at 402, 525 and 644 cm^{-1} corresponding to anatase phase TiO_2 in V_2O_5/TiO_2.[12] And the unsymmetrical peak appeared at bands 402, 525cm^{-1} was due to vanadium doping.[13]

Figure S8b shows the Raman spectra of different Si/Al ratio of HZSM-5 catalysts and also show different diffraction bands of vanadium species. It can be seen in the results that the diffraction band of 993 cm^{-1} in Si/Al=80 and Si/Al=35 is higher than Si/Al=50 which can cause more oxidation of the substrate. Moreover, when the Si/Al ratio comes 80, the diffraction band at 927 and 1031 cm^{-1} disappeared.

Tables

Table S1 Textural properties of the different supported catalysts with 2% loading of V_2O_5

Catalysts	BET surface areas (m^2g^{-1})	Pore diameter (nm)	Pore volume (cm^3g^{-1})
V_2O_5/HZSM-5	698.5	2.12	0.70
V_2O_5/MCM-41	1120.1	3.41	1.02
V_2O_5/SiO_2	459.8	2.21	0.47
V_2O_5/TiO_2	323.5	2.21	0.33

It can be seen from Table S1 that the BET surface area and pore volume of molecular sieve catalyst (V_2O_5/MCM-41 and V_2O_5/HZSM-5) is larger than the metal oxide supported catalyst (V_2O_5/SiO_2 and V_2O_5/TiO_2). Combined with XRD analysis, MCM-41 and HZSM-5 supported catalysts have a larger specific surface area, which is more beneficial for the uniform dispersion of vanadium species.

Table S2. The effect of 2% V_2O_5/HZSM-5 with different Si/Al ratio on catalytic performance

Entry	Raito	Conv	Yields (%)					
			NDA	1-naphthylamine	1,8-diaminonaphthalene	2, 3-diaminonaphthalene	1, 4-naphthoquinones	1-naphthol
1	35	30.10	24.75	4.58	trace	0.35	0.37	0.56
2	50	46.60	26.65	9.92	0.22	trace	0.23	0.69
3	80	31.54	24.10	4.10	2.89	trace	0.20	0.59

Reaction conditions: naphthalene 0.78 mmol; hydroxylamine hydrochloride 7.8 mmol; glacial acetic acid 15 ml; water 5 ml; reaction temperature 80 °C; reaction time 4 h.

As can be seen from the table, when the Si/Al ratio of HZSM-5 increased from 35 to 50, the naphthalene conversion is gradually increased. The 2% V_2O_5/HZSM-5 with a Si/Al ratio of 50 has the best catalytic performance, the yield of naphthylamine reaches to 36.79%. Combined with characterization, when the Si/Al=50, more Brönsted acid sites excite which leads to high yields. When the Si/Al ratio is too high, the acidity of the catalyst decrease, which affects the activation of hydroxylamine resulting in a decrease in catalytic effect.

Table S3. The amination of 1-naphthylamine to form 1,5- diaminonaphthalene

Rank	Conversion (%)	Selectivity (%)		
		NDA	1,8- diaminonaphthalene	1,4-naphthoquinone
1	37.80	57.40	0.00	7.20

Reaction conditions: 1-naphthylamine 0.01 mol; hydroxylamine hydrochloride 0.01 mol; glacial acetic acid 15 ml; water 5 ml; reaction temperature 80 °C; reaction time 4 h, 3%V_2O_5/HZSM-5 0.5g.

In order to clarify the relationship between 1,5- diaminonaphthalene and 1-naphthylamine synthesis, the substrate was replaced with 1-naphthylamine, and the amination experiment was carried out. The results show that 1-naphthylamine could also be converted to 1,5-diaminonaphthalene. Comparison of this result with the ratios of 1-naphthylamine/1,5-diaminonaphthalene obtained when naphthalene is used as the starting material (much more 1,5-diaminonaphthalene than 1-naphthylamine is obtained), it indicates that 1,5-diaminonaphthalene formation might not only from the 1-naphthylamine obtained in the reaction.

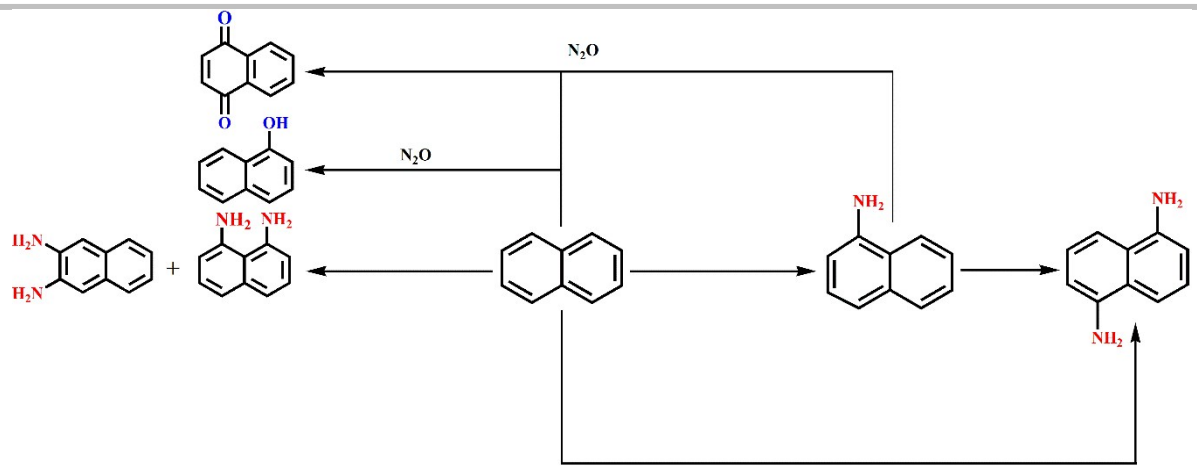

Scheme S1. The reaction path during naphthalene amination

Based on the experimental data, it could be proposed a possible reaction path (shown in **Scheme S1**) during naphthalene amination. Naphthylamine could be successfully synthesized by one-step naphthalene amination in the system of hydroxylamine and acid medium. The products included 1-naphthylamine, 1,5-diaminonaphthalene, 1,8-diaminonaphthalene, 2,3-diaminonaphthalene and slight amounts of the over oxidative products of 1,4-naphthoquinones and 1-naphthol. A small amount of hydroxylamine in the reaction system could be decomposed into N_2O within an oxidative environment, which leads to the formation of the oxidative products.

References

[1] a) C. Zhao, A. Johannes and Lercher, *Angew. Chem. Int. Ed.,* 2012, **31**, 5955-5940; b) F. Zhang, X. Ren and H. Huang, *Chin. J. Chem. Eng.,* 2018, **26**, 1031-1040.

[2] B. Schimmoeller, Y. Jiang, S. E. Pratsinis and, A. Baiker, *J. Catal.,* 2010, **274**, 64-75.

[3] H. Kosslick, G. Lischke, G. Walther, W. Storek and R. Fricke, *Microporous Mater.,* 1997, **9** :13‑33.

[4] Y. M. Liu, Y. Cao, N. Yi, W. L. Feng, W. L. Dai and S. R. Yan, *J. Catal.,* 2004, **224**, 417-428.

[5] H. Berndt, A. Martin, A. Brückner, E. Schreier, D. Müller and H. Kosslick, *J. Catal.,* 2000, **191**, 384-400.

[6] "The Handbook of Infrared and Raman Characteristic Frequencies of Organic Molecules": Lin-Vien, Daimay, *Academic Press,* 1991:155-189.

[7] Rodgers and G. Edward, *J. Chem. Phys.*, 1970, **52**, 4627.

[8] Zh. Luan, P. A. Meloni, R. S. Czernuszewicz and L. Kevan, *J. Phys. Chem.,* 1997, **101**, 9046-9051.

[9] G. Xiong, C. Li, H. Li, Q. Xin and Z. Feng, *Chem. Commun.,* 2000, **8**, 677-678.

[10] Bulánek, Roman, Cicmanec, Pavel and M. SetnicKa, *Phys. Procedia,* 2013, **44**, 195-205.

[11] A. Ali, I. Ruzybayev, E. Yassitepe, S. Ismat Shah and A.S. Bhatti, *J. Phys. Chem.,* 2013, **117**, 19517-19524.

[12] K. J. Reszka, M. Takayama, R. H. Sik, et al. *Photochem. Photobiol.*, 2005, **81**: 573-580.

[13] A. Z. Varzaneh, M. S Moghaddam and J. T. Darian, *Pet. Chem.,* 2018, **58**, 13-21.